A novel sensitive laccase biosensor using gold nanoparticles and poly L-arginine to detect catechol in natural water

Nasim Maleki[1]
Soheila Kashanian[1,2*]
Maryam Nazari[1,2]
Nahid Shahabadi[1,3]

[1]Faculty of Chemistry, Razi University, Kermanshah, Iran

[2]Nano Drug Delivery Research Center, Kermanshah University of Medical Sciences, Kermanshah, Iran

[3]Medical Biology Research Center, Kermanshah University of Medical Sciences, Kermanshah, Iran

Abstract

In this study, the simple, green, and fast layer-by-layer modification of the glassy carbon electrode was mainly performed by electrodeposition of gold nanoparticles and then, poly-L-arginine, and finally, laccase was covalently bonded to poly-L-arginine using glutaraldehyde. This type of fabrication is used for the first time for catechol detection, which provides a bioelectrocatalytic cycle for electron transport in the presence of laccase that results in sensitive and fast detection of catechol. The scanning electron microscopy, Fourier-transform infrared spectroscopy, and electrochemical studies were performed to confirm successful immobilization of the enzyme. The biosensor response was linear in a wide range of catechol trace concentrations, 24.90–274.00 nM, with the detection limit of 18.00 nM. Values of K_m, α, n, and K_s for the immobilized enzyme were calculated to be 1.25×10^{-2} μM, 0.56, 3.19, and 0.28 Sec^{-1}, respectively. It was examined in real sample successfully confirming it is capable of measuring catechol in natural water. Volume 66, Number 4, Pages 502–509, 2019

Keywords: *laccase, biosensor, catechol, poly L-arginine, AuNPs*

1. Introduction

Laccase (Lac) is a redox enzyme used as a biorecognition element in enzymatic biosensors to evaluate phenol and phenolic compounds in water and wastewater samples [1–3]. This enzyme belongs to the copper-containing oxidoreductases groups and is produced by fungi, plants, and bacteria [4, 5]. In the active site of Lac, there are four Cu atoms that are divided into three groups named as type 1 (T1), type 2 (T2), and type 3 (T3). T1 or blue copper is an approach to external enzyme sell, T2 or normal copper, and T3 or coupled binuclear copper form three nuclear centers that are responsible for the reduction of oxygen to water [6]. Lac can catalyze the oxidation of a wide range of phenolic substrates such as mono-phenols, di-phenols, polyphenols, methoxyphenols, and aminophenols with concomitant reduction of O_2 to water [7]. Therefore, Lac is applicable in different industries including biobleaching for the decolorization of dyes [8], chemical synthesis [9], bioremediation for the oxidation and removal of organic pollutants in water and wastewater [10, 11], and biosensing for the development of the phenolic compound biosensor [12–14].

Catechol is one of the phenolic compounds that has been widely used in medicine, cosmetics, dyes, and pesticides; it can also enter into groundwater from different sources [15]. The US Environmental Protection Agency (EPA) and the European Union (EU) consider it as an environmental pollutant due to its high toxicity to organisms [16]. Thus, catechol determination is very important in medicine, physiology, and also in environmental protection fields [17]. The common analytical techniques available to measure the concentration of phenol derivatives include spectrophotometry [18], capillary electrophoresis [19], liquid chromatography [20], and gas

Abbreviations: *DIW, deionized water; EPA, environmental protection agency; EU, European Union; FT-IR, Fourier-transform infrared spectroscopy; GCE, glassy carbon electrode; AuNPs, gold nanoparticles; Lac, Laccase; Arg, L-arginine; PArg, Poly-L-arginine; RSD, relative standard deviation; SEM, scanning electron microscopy; Ag/AgCl, Silver/silver-chloride.*

*Address for correspondence: Prof. Soheila Kashanian, Faculty of Chemistry, Razi University, Kermanshah, P.O. Box: 67149, Iran. Tel.: +988334274559; Fax: +988334274559; e-mail: kashanian_s@yahoo.com.

Received 19 January 2019; accepted 24 March 2019

DOI: 10.1002/bab.1746

Published online 5 April 2019 in Wiley Online Library (wileyonlinelibrary.com)

chromatography [21]. However, these techniques are time-consuming, unportable, and expensive. Moreover, they need skilled operators and preconcentration steps.

Biosensors, on the other hand, are more advantageous because they are cost effective, fast, portable, and they do not require trained operators [22]. Due to low stability and weak reusability, Lac should be immobilized by an effective method [23]. Immobilization is a key step in the fabrication of a biosensor [24]. There are different ways that can be used to immobilize Lac, such as entrapment by the three-dimensional matrix [25], encapsulation by organic or inorganic polymer [26], adsorption by solid supports [27], and covalent binding of functional groups containing carriers [28]. The best immobilization method is covalent bonding due to its advantages including long-term stability and prevention from enzyme leakage; also, in this study, it was used for immobilization of Lac.

Electropolymerization is a good choice to create a conductive surface with functional groups for the immobilization of enzymes [29]. Amino acids like arginine can be electropolymerized and used on the surface of biosensors for the detection of drugs, dopamine, uric acid, ascorbic acid, and other analytes [30]. L-Arginine (Arg) is zwitterion and has COOH and NH_2 functional groups, and thus it is used for the electrostatic or covalent binding immobilization method.

Gold nanoparticles (AuNPs) are among the most studied nanomaterials due to some remarkable properties such as large specific surface area, high electrochemical catalytic activity, strong adsorption ability, biocompatibility, well suitability, and good conductivity. AuNPs have been successfully used to synthesize different types of optical, electrochemical sensors, and biosensors [31, 32]. Employing of AuNPs on the electrode surface provides higher current signals that is the result of much larger surface area; also, it can affect electron transport due to contact between AuNPs and biologic element; in addition, the selectivity, robustness, and sensitivity can be improved [33–35].

In this study, Lac was immobilized onto modified glassy carbon electrode (GCE) (PArg/AuNPs/GCE) surface through the covalent binding between NH_2 groups of Lac and poly-L-arginine (PArg) using glutaraldehyde for the voltammetric measurement of catechol in natural water. This biosensor provides a good Lac immobilized surface with highly improved electrocatalytic efficiency, selectivity, sensitivity, storage, reusability, and stability.

2. Material and Methods

2.1. Materials and reagents

$HAuCl_4$, catechol, Arg, phenol, catechin, aminophenol, $K_3Fe(CN)_6$, and Lac (EC 1.10.3.2, from *Trametes Versicolor*, 20.48 U/mg) were purchased from Sigma–Aldrich, St. Louis, MO, USA. Na_2HPO_4 and NaH_2PO_4 were bought from BDH, Poole, England. The used supporting electrolyte was phosphate buffer solution. Deionized water (DIW) was used to prepare all aqueous solutions.

2.2. Apparatus

The layers morphologies were studied by a Hitachi scanning electron microscopy (SEM) (SU1510). Before the SEM process, the AuNPs/GCE-, PArg/AuNPs/GCE-, and Lac/PArg/AuNPs/GCE-modified electrodes were sputter coated with gold for 90 Sec. The electrochemical experiments were accomplished at room temperature by electro analyzer system (Sama 500). A three-electrode cell with a platinum auxiliary electrode, a GCE (3.0 mm in diameter), and a silver/silver-chloride (Ag/AgCl) reference electrode were employed for the electrochemical evaluations.

2.3. Fabrication of Lac/PArg/AuNPs/GCE biosensor

The reason for choosing AuNPs and PArg was to manufacture a highly conductive layer-by-layer platform to covalently bond the enzyme above it.

First, the GCE was cleaned with water and varnished by a polishing cloth, followed by polishing the bare electrode by diamond paste, and rinsing thoroughly by DIW. Finally, the electrode was dried. Then, AuNPs were deposited on the GCE surface by electrochemically treating the electrode at the constant potential of −0.2 V (vs. Ag/AgCl) for 300 Sec, which was being immersed in a solution containing $AuHCl_4$ (4.60 mM) and $NaNO_3$ (0.10 M) [36]. Next, the electrode was rinsed gently with DIW to remove the physically absorbed $HAuCl_4$ and $NaNO_3$. To create positively charged PArg, the cyclic voltammetry technique was employed from −2.00 to +2.50 V at 100 mV Sec^{-1} scan rate for 10 cycles in a solution of phosphate buffer (1 mL, 0.03 M) and Arg (6.00 mL, 0.10 M) [37]. After rinsing the electrode with ultrapure water, 5 μL of glutaraldehyde (0.50%, v/v) was dropped on the prepared electrode and air dried. Finally, 10 μL of negatively charged Lac solution (1 mg/mL, phosphate buffer pH 6) was sprayed above the previously constructed layers to obtain Lac/PArg/AuNPs/GCE. The constructed electrode was kept at 4 °C when not in use.

3. Results and Discussions

Different features of the modified electrode were revealed by several experiments. To evaluate the surface structure and morphology, Fourier-transform infrared spectroscopy (FT-IR) measurements and SEM were performed, respectively. Electrochemical surface areas of the bare and modified electrodes were compared using cyclic voltammetry technique, and catechol detection was tested similarly. The optimized pH condition was specified, and enzyme activity was calculated. Different scan rates were employed to clarify the reaction mechanism. Eventually, biosensing performance of the Lac/PArg/AuNPs/GCE was explored, and natural water was used to verify the practical use of the proposed biosensor. All the corresponding results are discussed below.

3.1. Characterization of Lac/PArg/AuNPs/GCE

Cyclic voltammetry experiments were performed to investigate the electrochemical properties of the modifying layers, using 5 mM $K_3[Fe(CN)_6]$ and 0.1 M KCl solution as a redox probe.

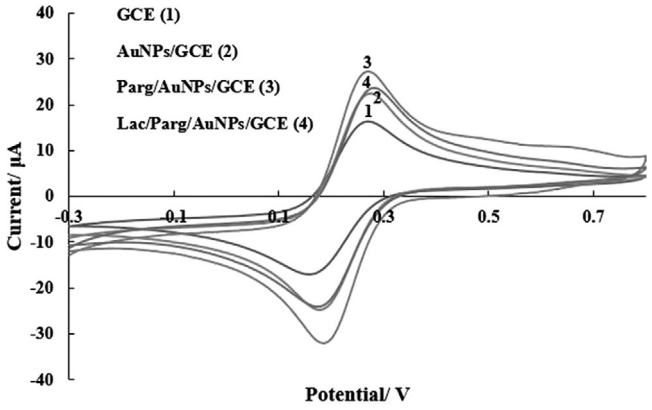

FIG. 1 *CVs of the GCE (1), AuNPs/GCE (2), PArg/AuNPs/GCE (3), and Lac/PArg/AuNPs/GCE (4) in 5 mM $K_3[Fe(CN)_6]$ and KCl 0.1 M solution.*

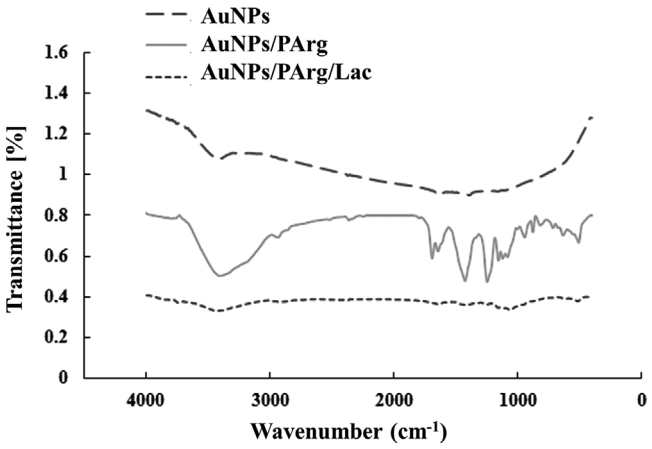

FIG. 2 *FT-IR spectrum of AuNPs/GCE, PArg/AuNPs/GCE, and Lac/PArg/AuNPs/GCE.*

Fig. 1 shows the obtained voltammograms. A pair of well-defined redox peaks is observed at the bare GCE (curve 1). The redox peaks increased by modifying the GCE with AuNPs (curve 2), which is attributed to the excellent conductivity of these nanoparticles [38]. After electropolymerizing Arg on the modified electrode, the achieved voltammogram (curve 3) showed higher peak currents, owing to the positive charge of PArg, which accelerates the reaction of $[Fe(CN)_6]^{3-}$ [39]. By adding the Lac enzyme on top of PArg/AuNPs/GCE, the anodic and cathodic currents decrease due to hindered diffusion of $[Fe(CN)_6]^{3-}$ by the negatively charged enzymes.

FT-IR studies were conducted to further investigate the prepared biosensor structure. The obtained results are presented in Fig. 2. The peak for hydrxoy group is observed at about 3,200 cm^{-1}, which is seen in the spectrum of AuNPs and all the subsequent spectra. Also, the bands at about 1,680 cm^{-1} for the amide I stretching, 1,600 cm^{-1} for the amine group bending, 1,040 and 3,400 cm^{-1} for the primary amine group stretching show the successful synthesis of PArg [40]. The bands are seen in the next two spectra. By adding glutaraldehyde to the PArg/AuNPs/GCE structure and then adding the Lac enzyme, some bonds were created between the amine groups of the enzyme and the amine groups of PArg. As a result, the intensity of the peaks related to the primary amine groups are decreased in the FT-IR spectrum of the final biosensor setup. The FT-IR analyses proved that the layer-by-layer structure was successfully prepared.

The morphologies of AuNPs/GCE, PArg/AuNPs/GCE, and Lac/PArg/AuNPs/GCE were examined by the SEM. Figure 3a depicts the formation of AuNPs on the surface of the GCE. Similarly, as shown in Fig. 3b, the electropolymerization of Arg formed a thick layer on the AuNPs, which is in accordance with the literature [40]. The last layer of the whole structure was built by linking the concentrated solution of Lac to the amine groups of PArg. Figure 3c displays where the enzyme layer fully covered PArg. SEM images show the successful layer-by-layer structure and enzyme immobilization.

3.2. Electrochemical surface area

The areas of Lac/PArg/AuNPs/GCE and the bare GCE were calculated by performing cyclic voltammetry in 5 mM $K_3[Fe(CN)_6]$, at various scan rates. The following Randles–Sevcik equation was used for a reversible process [41]:

$$I_{pa} = \left(2.69 \times 10^5\right) n^{1.5} A_0 D_0^{0.5} C_0 \nu^{0.5} \quad (1)$$

where I_{pa} is the peak current of the anode, the number of transferred electrons is n, A_0 refers to the electrode area, D_0 is the diffusion coefficient, $K_3[Fe(CN)_6]$ concentration is shown by C_0, and the scan rate by ν. For $K_3[Fe(CN)_6]$ solution (5.0 mM, 0.10 M KCl), $n = 1.00$ and $D_0 = 7.60 \times 10^6$ cm^2 Sec^{-1}; the slope of the plot I_{pa} versus $\nu^{0.5}$ was computed to determine the effective surface area. For the GCE and AuNPs/PArg/Lac/GCE, the slopes were 0.13 A (V $Sec^{-1})^{-0.5}$ and 0.29 A (V $Sec^{-1})^{-0.5}$, respectively. Accordingly, the areas of the electrodes were 3.54×10^{-2} and 7.89×10^{-2} cm^2 for the bare and modified (Lac/PArg/AuNPs/GCE) electrodes, respectively. The obtained results show that the biosensor has 2.22 times larger surface area than the bare GCE.

3.3. Electrochemical behavior of catechol at Lac/PArg/AuNPs/GCE

Figure 4 presents the cyclic voltammetry of various electrodes in 1.00 mM catechol solution (0.10 M phosphate buffer, pH 6.00) and the final biosensor setup in the solution of phosphate buffer (0.10 M, pH 6.0). The oxidation/reduction peaks related to catechol reaction can be seen on GCE (Fig. 4, line 1), whereas in the cyclic voltammetries of the other modifications such as AuNPs/GCE (Fig. 4, line 2) and PArg/AuNPs/GCE (Fig. 4, line 3), the redox peaks are not clear. However, owing to the excellent conductivity and the improved electrode surface area Lac/PArg/AuNPs/GCE (Fig. 4, line 4) depicts high redox peak currents and small peak-to-peak potential separation. The sensitivity of the prepared electrode, Lac/PArg/AuNPs/GCE, toward catechol was checked by cyclic voltammetry in phosphate buffer (0.10 M, pH 6.00) and the obtained result is illustrated in Fig. 4,

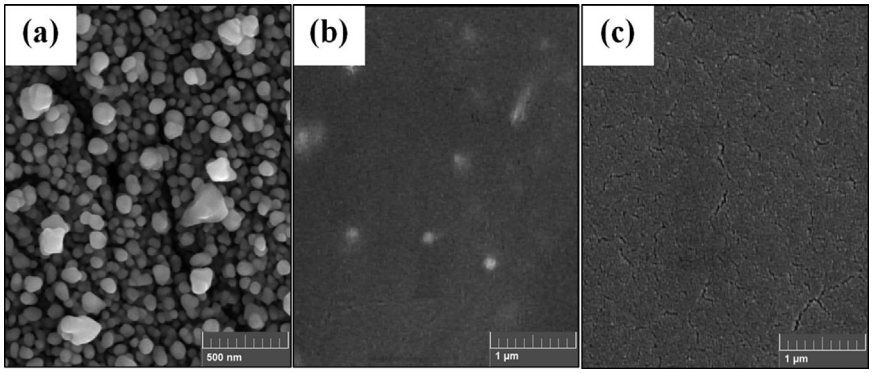

FIG. 3 *The SEM image of (a) AuNPs/GCE, (b) PArg/AuNPs/GCE, and (c) Lac/PArg/AuNPs/GCE.*

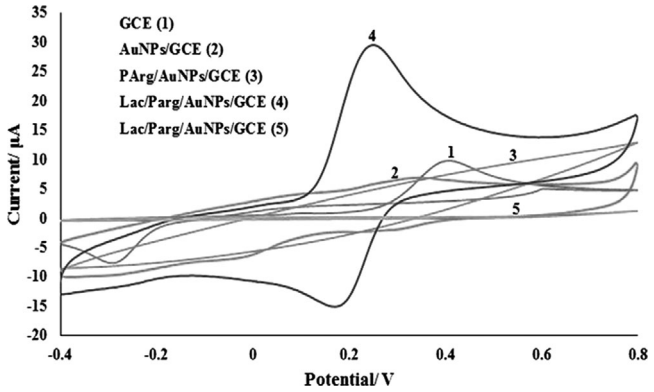

FIG. 4 *CVs of catechol at GCE (1), AuNPs/GCE (2), PArg/AuNPs/GCE (3), and Lac/PArg/AuNPs/GCE (4) in catechol 1.00 mM and phosphate buffer (0.10 M, pH 6.00) and Lac/PArg/AuNPs/GCE (5) in phosphate buffer (0.10 M, pH 6.00).*

line 5. The evaluation of the curves for Lac/PArg/AuNPs/GCE (Fig. 4, line 4) and Lac/PArg/AuNPs/GCE (Fig. 4, line 5) indicates that catechol redox peaks are observed when catechol is present in the buffer. Figure 4 depicts the redox peak potentials at 0.25 and 0.17 V (vs. Ag/AgCl). The formal potential ($E^{0\prime}$) is ca. 0.21 V and ΔE_p is 73.00 mV at 100 mV Sec^{-1} scan rate, resulting in a rapid electron transfer. The value of ΔE_p was high for a reversible system, (59/n) mV. Thereupon, the catechol redox reaction is a quasi-reversible reaction [42, 43].

3.3.1. pH effect

The solution pH has a huge impact on the electrochemical reaction. To distinguish the optimal operating condition, the pH effect was studied by the cyclic voltammetry from −0.10 to 0.60 V and at ν equal to 100 mV Sec^{-1} (Fig. 5a). The maximum cathodic peak current was generated at pH 6 illustrating that the enzyme activity is higher at this pH level. The cathodic peak potential was also influenced by the pH of the solution; an increase in pH shifted the values of the cathodic peak potential to negative potentials (Fig. 5b), illustrating the protons contribution in the electrochemical reaction [2]. The plot of E_{pc} versus pH was linear, and the slope was −37.90 mV pH^{-1} ($R^2 = 0.9824$), suggesting a two-electron, one-proton reduction process [44, 45]. The obtained data from Figs. 5b and 5c declare that cathodic peak current is higher at pH 6 and ΔE_p is lower at the same pH level, resulting in better sensitivity and rapid electron transfer. Accordingly, the pH 6 was selected as the best operation pH and employed in the subsequent tests.

3.3.2. Assay of enzyme activity

To monitor the enzyme–substrate reaction and the affinity of Lac–catechol, activity assay was fulfilled in various reaction mixtures. The mixtures contained free enzyme and catechol with different concentrations of 0.75–2.50 mM in the solution of 0.10 M phosphate buffer, adjusted to pH 6.00. UV–vis spectroscopy was utilized to monitor the changes in substrate concentrations. Similarly, for the immobilized Lac, the changes in the cathodic peak currents were studied by cyclic voltammetry. The obtained data (Fig. 6) resembled the Michaelis–Menten pattern; subsequently, the following formulas were used to evaluate the enzyme activity of the immobilized and free Lac [46]:

$$A_c = \frac{A_{c,max} C}{K_m + C} \tag{2}$$

$$I_{p,c} = \frac{I_{p,max} C}{K_m^{app} + C} \tag{3}$$

where A_c is the absorbance change per minute, *C is* substrate concentration, $A_{c,max}$ is the maximum absorbance change, K_m is Michaelis−Menten constant. $I_{p,c}$ is the peak current, $I_{p,max}$ is the maximum generated current when the substrate concentration is saturated, $K_m{}^{app}$ is the apparent Michaelis−Menten constant. K_m and $K_m{}^{app}$ were 4.86×10^{-2} and 1.25×10^{-2} µM for free and covalently bonded enzymes, respectively. $K_m{}^{app}$ is smaller for the immobilized enzyme, and this reveals that the immobilized Lac on Lac/PArg/AuNPs /GCE possessed higher affinity and enzymatic activity for catechol [2].

3.3.3. Effect of the scan rate

The behavior mechanism of the electron transfer for the proposed biosensor is as follows: catechol is oxidized to the homologous 1,2-benzoquinone by the oxidized form of Lac,

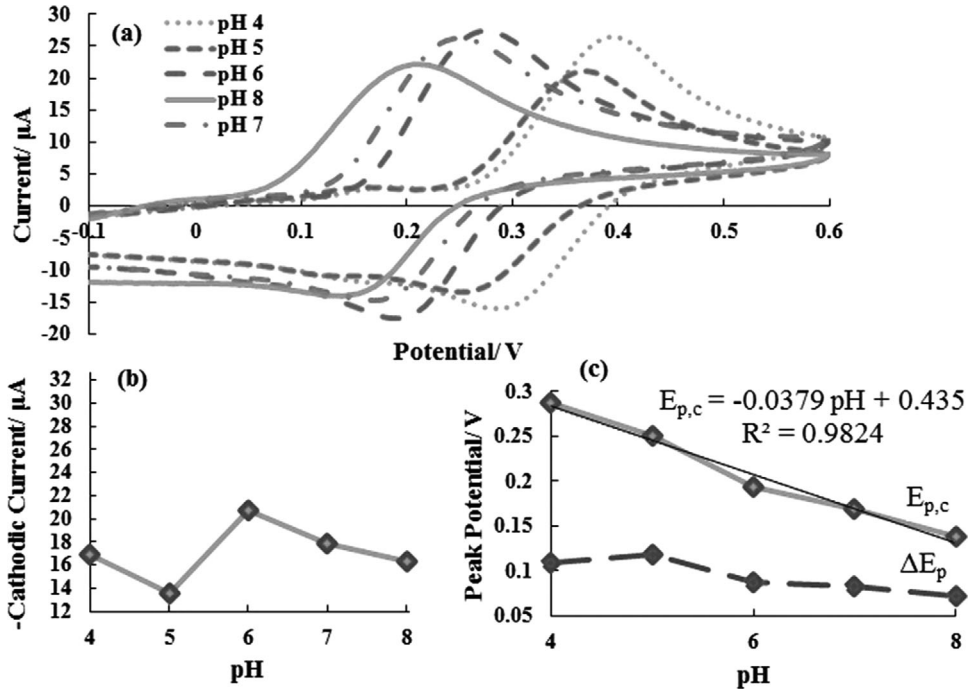

FIG. 5 *pH effect on (a) catechol biosensing for Lac/PArg/AuNPs/GCE in catechol 1.00 mM and phosphate buffer (0.10 M). (b) Cathodic peak currents changes with pH. (c) Cathodic peak potentials and peak-to-peak separation changes with pH.*

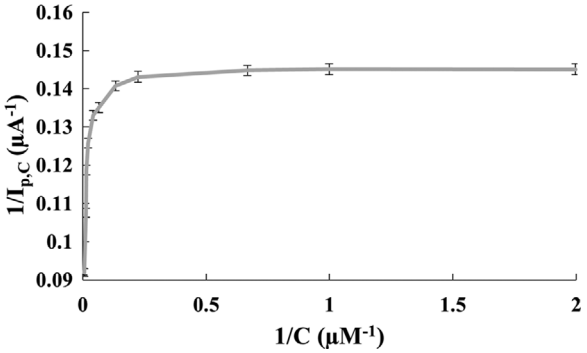

FIG. 6 *Michaelis–Menten behavior of the Lac-catechol.*

after which the reduced form of Lac releases the electrons to returen to its oxidized form. Then, a cycle (bioelectrocatalytic) is followed, and the produced electrons passed on to the working electrode [47–49].

In this study, scan rate variation (v) affected the redox peak currents. Lac/PArg/AuNPs/GCE was immersed in 1.00 mM catechol (phosphate buffer 0.10 M, pH 6.00) and the experiments were accomplished in different scan rates. An increase in the scan rate, shifted the E_{pa} positively and the E_{pc} negatively. Moreover, the potential scan rate and redox peak currents were in a linear relationship from 40 to 100 mV Sec^{-1}; demonstrating that the redox reactions were controlled by adsorption (Fig. 7a) [50–52].

The regression equations between the potential scan rate and the redox peak currents are I_{pc} (µA) $= -0.0921v$ (mV Sec^{-1}) $- 7.6690$ ($R^2 = 0.9868$) and I_{pa} (µA) $= 0.0870v$ (mV Sec^{-1}) $+ 8.5632$ ($R^2 = 0.9816$). The peak-to-peak potential separation (ΔE_p) increased gradually by increasing the scan rate. Consequently, the Laviron's equations were used to compute the electrochemical parameters [53]:

$$E_{pa} = E^{o'} + \frac{2.303RT}{(1-\alpha)nF}\log v + \frac{2.303RT}{(1-\alpha)nF}\log\frac{nF(1-\alpha)}{RTk_s} \quad (4)$$

$$E_{pc} = E^{o'} - \frac{2.303RT}{\alpha nF}\log v - \frac{2.303RT}{\alpha nF}\log\frac{nF\alpha}{RTk_s} \quad (5)$$

$$\log k_s = \alpha\log(1-\alpha) + (1-\alpha)\log\alpha - \log\frac{2.303RT}{nFv} - \frac{\alpha(1-\alpha)nF\Delta E_p}{2.3RT} \quad (6)$$

where n is the number of electrons transferred, k_s is the apparent heterogeneous electron transfer rate constant, and α is the charge transfer coefficient. The obtained equations are E_{pa} (mV) $= 42.0870 \log v$ (mV Sec^{-1}) $+ 218.9500$ ($R^2 = 0.9876$) and E_{pc} (mV) $= -33.1720 \log v$ (mV Sec^{-1}) $+ 258.9600$ ($R^2 = 0.9841$) (Fig. 7b). α, k_s, and n were 0.56, 0.28 Sec^{-1}, and 3.19, respectively.

3.3.4. Analytical performance

Catechol quantification by Lac/PArg/AuNPs/GCE was fulfilled using the enzymatic reduction of catechol. The relationship between catechol concentration and the peak current was evaluated by the differential pulse voltammetry, Fig. 8 (inset).

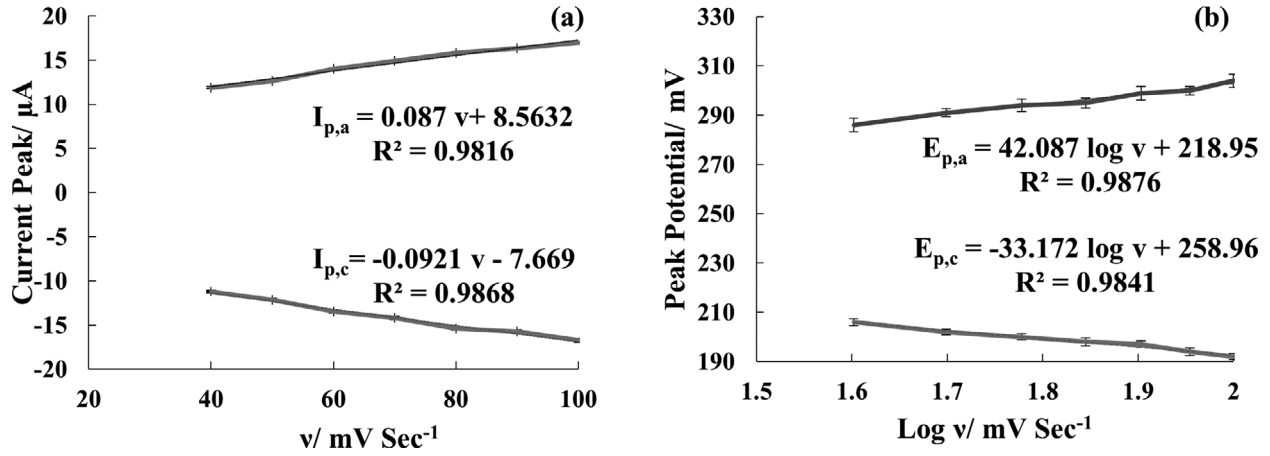

FIG. 7

Scan rate effect. (a) Redox peak currents changes versus scan rate from 40 to 100 mV Sec^{-1} (0.001 M catechol and phosphate buffer 0.10 M, pH 6.00). (b) Redox peak potentials changes versus scan rate from 40 to 100 mV Sec^{-1} (1.00 mM catechol and phosphate buffer 0.10 M, pH 6.00).

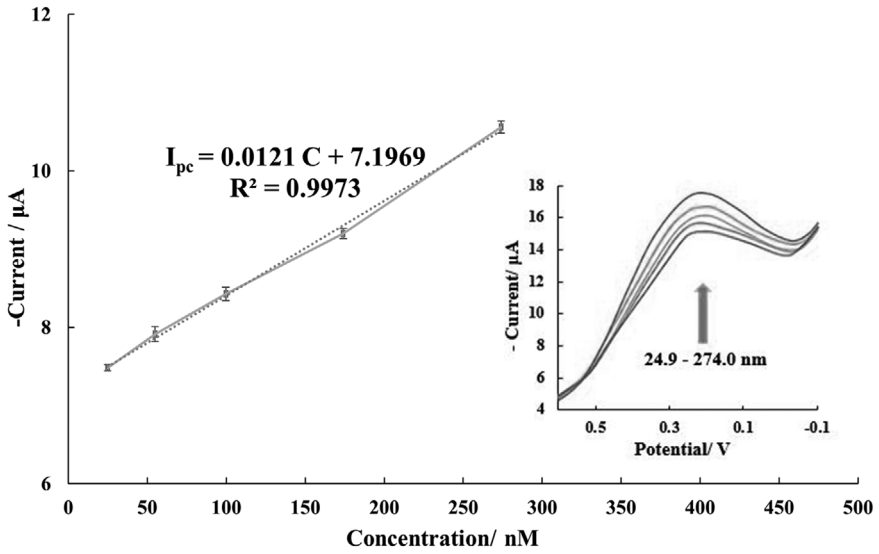

FIG. 8

Relationship of current responses to catechol concentration from 24.90 to 274.00 nM. Inset: The differential pulse voltammetry responses of Lac/PArg/AuNPs/GCE to various catechol concentration 24.90, 49.00, 99.70, 174.00, and 274.00 nM in 0.10 M phosphate buffer (pH 6.00) (n = 3).

This process was repeated three times, and the mean results were used to obtain the biosensor calibration curve. The relative standard deviation (RSD) for all the tested points was less than 2%.

If the catechol concentration ranges from 24.90 to 274.00 nM (room temperature and pH 6.00), the cathodic peak current and the catechol concentration indicate a linear relationship (Fig. 8). The regression equation is: I_{pa} (µA) = 0.0121C (nM) + 7.1969 (R^2 = 0.9973) ranging from 24.90 to 274.00 nM. The detection limit was 18.00 nM. The obtained results from this work and other researchs are presented in Table 1. The proposed biosensor has a low detection limit (nanomolar range), and it can be used for very sensitive samples with low concentrations of catechol. As can be seen, in Table 1, it has the best sensitivity in comparison with other biosensors. In addition, it showed the lowest K_m^{app}, which revealed that the proposed biosensor demonstrated higher affinity for enzymatic activity compared with other biosensors.

3.4.5. Reproducibility, selectivity, recovery study, and analytical application

Fifteen successive measurements were performed using one modified electrode to detect catechol in a phosphate buffer

TABLE 1 *Comparison of catechol detection obtained by several Lac-modified electrodes*

Modified electrode	*Sensitivity ($\mu A\ \mu M^{-1}$)*	*Linear range (μM)*	*LOD (μM)*	*K_m^{app} (μM)*	*K_s (Sec^{-1})*	*References*
Lac/PANI/GCE	7.06×10^{-1}	3.20 to $1.96 \times 10^{+1}$	2.07	_	_	[52]
P3MT-LAC/GCE	_	8.00×10^{-2} to $1.40 \times 10^{+1}$	1.00×10^{-2}	7.60	_	[54]
PDA-Lac-NiCNFs/MGCE	2.50×10^{-2}	1.00 to $9.10 \times 10^{+3}$	6.90×10^{-1}	$7.80 \times 10^{+3}$	1.79	[2]
PEDOT-rGO-Fe_2O_3-PPO/GCE	_	4.00×10^{-2} to $6.2 \times 10^{+1}$	7.00×10^{-3}	$3.04 \times 10^{+1}$	_	[55]
Tyr-AuNPs-DHP/GCE	_	2.50 to $9.50 \times 10^{+1}$	1.70×10^{-1}	_	_	[56]
Lac/PArg/AuNPs/GCE	$1.21 \times 10^{+1}$	2.49×10^{-2} to 2.74×10^{-1}	1.80×10^{-2}	1.25×10^{-2}	2.82×10^{-1}	This work

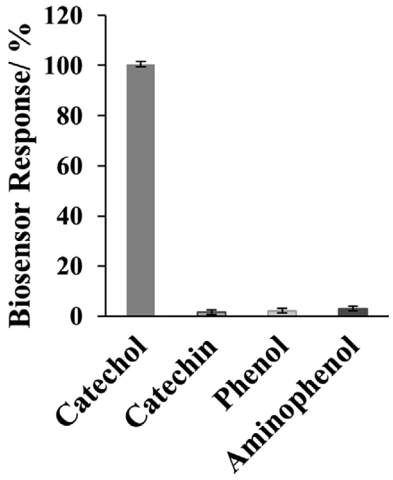

FIG. 9 *Relative responses of Lac/PArg/AuNPs/GCE for a mixture of different phenolic compounds (catechol, catechin, phenol, aminophenol; 25.00 nM in pH 6.00 phosphate buffer solution).*

solution (0.10 M, pH 6.00) containing 25.00 nM catechol. The modified electrode exhibited good reproducibility by RSD of the cathodic peak current being 1.46% [54, 57].

The selectivity of biosensor was done in the mixture of structurally similar molecules to catechol. So, catechol and some phenol derivatives, such as catechin, phenol, and aminophenol (25.00 nM in phosphate buffer 0.10 M, pH 6.00) were employed to evaluate the biosensor selectivity. Figure 9 demonstrates that catechol has the highest signal of 100%. However, other derivatives show almost no response.

Samples from Gharesu river and tap water were spiked with catechol and used to study the recovery and practical applications of the biosensor. Before the experiments, the phosphate buffer solution (0.10 M, pH 6.00) was used to dilute all the samples (20 times), to fit the calibration curve [2]. Next, 25.00 nM catechol solutions were prepared to be detected by the differential pulse voltammetry technique at Lac/PArg/AuNPs/GCE. The test was performed three times. The results are gathered in Table 2. The recoveries show acceptable accuracy, confirming that the developed biosensor is capable of measuring catechol in natural water.

TABLE 2 *Recovery study and catechol detection of Lac/PArg/AuNPs/GCE in water samples (n = 3)*

Sample type	*Catechol spiked (nM)*	*Catechol found (nM)*	*Recovery (%)*	*RSD%*
Tap water	25.00	25.48	101.93	
Tap water	25.00	25.85	103.40	1.30
Tap water	25.00	25.2	100.80	
Gharesu river	25.00	26.45	105.80	
Gharesu river	25.00	25.5	102.00	1.83
Gharesu river	25.00	25.9	103.60	

4. Conclusions

In the present study, a novel and highly sensitive Lac biosensor was developed to detect catechol in natural water. The electropolymerization of green materials was used as the main technique to prepare the modified electrode fast. It was observed that the covalently bonded Lac showed very good biocatalytic activity toward the reduction of catechol and the layer-by-layer structure of the biosensor Lac/PArg/AuNPs/GCE provided a great tool to detect catechol in trace values in a wide linear range with high selectivity and sensitivity. The biosensor was successfully tested for catechol detection in natural water samples. Very low detection limit, wide linear range, good reproducibility, and easy construction method approve that this modified electrode is a strong candidate for practical applications.

5. References

[1] Rodríguez-Delgado, M., and Ornelas-Soto, N. (2017). Green Technologies and Environmental Sustainability, Springer, pp. 45–65.
[2] Li, D., Luo, L., Pang, Z., Ding, L., Wang, Q., Ke, H., Huang, F., and Wei, Q. (2014) ACS Appl. Mater. Interfaces 6, 5144–5151.
[3] Karim, F., and Fakhruddin, A. (2012) Crit. Rev. Environ. Sci. Technol. 11, 261–274.
[4] Yang, Y., Ding, Y., Liao, X., and Cai, Y. (2013) Process Biochem. 48, 351–357.
[5] Majumdar, S., Lukk, T., Solbiati, J.O., Bauer, S., Nair, S.K., Cronan, J.E., and Gerlt, J.A. (2014) Biochemistry, 53, 4047–4058.
[6] Martínez-Sotres, C., Rutiaga-Quiñones, J.G., Herrera-Bucio, R., Gallo, M., and López-Albarrán, P. (2015) Wood Sci. Technol. 49, 857–868.
[7] Vignesh, R., Madhusudhanan, J., Gandhiraj, V., and Deepika, R.C. (2016) Int. Res. J. Eng. Technol. 3, 2499–2502.
[8] Mohajershojaei, K., Mahmoodi, N.M., and Khosravi, A. (2015) Biotechnol. Bioprocess Eng. 20, 109–116.
[9] Otrokhov, G.V., Shumakovich, G.P., Khlupova, M.E., Vasil'eva, I.S., Kaplan, I.B., Zaitchik, B.T., Zaitseva, E.A., Morozova, O.V., and Yaropolov, A.I. (2016) RSC Adv. 6, 60372–60375.
[10] Asadgol, Z., Forootanfar, H., Rezaei, S. Mahvi, A.H., and Faramarzi, M.A. (2014) J. Environ. Health Sci. Eng. 12, 93–98.
[11] Becker, D., Rodriguez-Mozaz, S., Insa, S., Schoevaart, R., Barceló, D., De Cazes, M., Belleville, M.-P., Sanchez-Marcano, J., Misovic, A., and Oehlmann, J.r. (2017) Org. Process Res. Dev. 21, 480–491.
[12] Casero, E., Petit-Domínguez, M., Vázquez, L., Ramírez-Asperilla, I., Parra-Alfambra, A., Pariente, F., and Lorenzo, E. (2013) Talanta 115, 401–408.
[13] Lepore, M., and Portaccio, M. (2016) Biotechnol. Appl. Biochem. 64, 782–792.
[14] Fogel, R., and Limson, J. (2016) Biosensors 6, 5–22.
[15] Nazari, M., Kashanian, S., Moradipour, P., and Maleki, N. (2018) J. Electroanal. Chem. 812, 122–131.
[16] Karim-Nezhad, G., Moghaddam, M.H., Khorablou, Z., and Dorraji, P.S. (2017) J. Electrochem. Soc. 164, B193-B199.
[17] Qu, J., Lou, T., Wang, Y., Dong, Y., and Xing, H. (2015) Anal. Lett. 48, 1842–1853.
[18] Sun, R., Wang, Y., Ni, Y., and Kokot, S. (2014) J. Hazard. Mater. 266, 60–67.
[19] Maringer, L., Ibáñez, E., Buchberger, W., Klampfl, C.W., and Causon, T.J. (2015) Electrophoresis 36, 348–354.
[20] Sergiel, I., Pohl, P., and Biesaga, M. (2014) Food Chem. 145, 404–408.
[21] Schmidt, L., Müller, J., and Göen, T. (2013) Anal. Bioanal. Chem. 405, 2019–2029.
[22] Rapini, R., and Marrazza, G. (2016) Compr. Anal. Chem. 74, 3–31.
[23] Xu, R., Chi, C., Li, F., and Zhang, B. (2013) ACS Appl. Mater. Interfaces 5, 12554–12560.
[24] Fartas, F.M., Abdullah, J., Yusof, N.A., Sulaiman, Y., and Saiman, M.I. (2017) Sensors 17, 1132–1146.
[25] Guzik, U., Hupert-Kocurek, K., and Wojcieszyńska, D. (2014) Molecules 19, 8995–9018.
[26] Zhang, C., Hu, C., Zhao, Y., Möller, M., Yan, K., and Zhu, X. (2013) Langmuir 29, 15457–15462.
[27] Tavares, A.P., Silva, C.G., Dražić, G., Silva, A.M., Loureiro, J.M., and Faria, J.L. (2015) J. Colloid Interface Sci. 454, 52–60.
[28] de Souza Bezerra, T.M., Bassan, J.C., de Oliveira Santos, V.T., Ferraz, A., and Monti, R. (2015) Process Biochem. 50, 417–423.
[29] Soylemez, S., Hacioglu, S.O., Kesik, M., Unay, H., Cirpan, A., and Toppare, L. (2014) ACS Appl. Mater. Interfaces 6, 18290–18300.
[30] Hasanzadeh, M., Mokhtari, F., Shadjou, N., Eftekhari, A., Mokhtarzadeh, A., Jouyban-Gharamaleki, V., and Mahboob, S. (2017) Mater. Sci. Eng. C 75, 247–258.
[31] Lanzellotto, C., Favero, G., Antonelli, M., Tortolini, C., Cannistraro, S., Coppari, E., and Mazzei, F. (2014) Biosens. Bioelectron. 55, 430–437.
[32] Yang, Y., Asiri, A.M., Du, D., and Lin Y. (2014) Analyst 139, 3055–3060.
[33] Qin, L., Zeng, G., Lai, C., Huang, D., Xu, P., Zhang, C., Cheng, M., Liu, X., Liu, S., Li, B., and Yi, H. (2018) Coord. Chem. Rev. 359, 1–31.
[34] Qin, L., Huang, D., Xu, P., Zeng, G., Lai, C., Fu, Y., Yi, H., Li, B., Zhang, C., Cheng, M., Zhou, C., and Wen, X. (2019) J. Colloid Interface Sci. 534, 357–369.
[35] Qin, L., Zeng, G., Lai, C., Huang, D., Zhang, C., Xu, P., Hu, T., Liu, X., Cheng, M., Liu, Y., Hu, L., and Zhou, Y. (2017) Sens. Actuators B Chem. 243, 946–954.
[36] Zhang, K., Ma, H., Zhang, L., and Zhang, Y. (2008) Electroanalysis 20, 2127–2133.
[37] Cao, Q., Zhao, H., Yang, Y., He, Y., Ding, N., Wang, J., Wu, Z., Xiang, K., and Wang, G. (2011) Biosens. Bioelectron. 26, 3469–3474.
[38] Li, T., Yao, T., Zhang, C., Liu, G., She, Y., Jin, M., Jin, F., Wang, S., Shao, H., and Wang, J. (2016) RSC Adv. 6, 66949–66956.
[39] Li, Y., Ye, Z., Zhou, J., Liu, J., Song, G., Zhang, K., and Ye, B. (2012) J. Electroanal. Chem. 687, 51–57.
[40] Zhang, F., Wang, Z., Zhang, Y., Zheng, Z., Wang, C., Du, Y., and Ye, W. (2012) Talanta 93, 320–325.
[41] Alwarappan, S., Liu, C., Kumar, A., and Li, C.-Z. (2010) J. Phys. Chem. C 114, 12920–12924.
[42] Li, Y., Zhang, L., Li, M., Pan, Z., and Li, D. (2012) Chem. Cent. J. 6, 103–111.
[43] Bard, A.J., and Faulkner, L.R. (2001). Fundamentals and applications, Electrochemical Methods 2.
[44] Fei, J., Wu, K., Yi, L., and Li, J. (2005) Bull. Korean Chem. Soc. 26, 1403–1409.
[45] Mollarasouli, F., Asadpour-Zeynali, K., Campuzano, S., Yáñez-Sedeño, P., and Pingarrón, J.M. (2017) Electrochim. Acta 246, 303–314.
[46] Portaccio, M., Di Martino, S., Maiuri, P., Durante, D., De Luca, P., Lepore, M., Bencivenga, U., Rossi, S., De Maio, A., and Mita, D. (2006) J. Mol. Catal. B Enzym. 41, 97–102.
[47] Zheng, Y., Wang, D., Li, Z., Sun, X., Gao, T., and Zhou, G. (2018) Colloids Surf. A 538, 202–209.
[48] Nazari, M., Kashanian, S., Maleki, N., and Shahabadi, N. (2019) Bull. Mater. Sci. 42(2): 42–51.
[49] Li, Z., Zheng, Y., Gao, T., Liu, Z., Zhang, J., and Zhou, G. (2018) J. Mater. Sci. 53(11), 7996–8008.
[50] Rafipour, R., Kashanian, S., Hashemi, S., Shahabadi, N., and Omidfar, K. (2016) Biotechnol. Appl. Biochem., 63, 740–745.
[51] López, B.P., and Merkoçi, A. (2009) Analyst 134, 60–64.
[52] Nazari, M., Kashanian, S., and Rafipour, R. (2015) Spectrochim. Acta A Mol. Biomol. Spectrosc. 145, 130–138.
[53] Laviron, E. (1979) Biotechnol. Appl. Biochem. J. Electroanal. Chem. Interfacial Electrochem. 101,19-28.
[54] Sethuraman, V., Muthuraja, P., Sethupathy, M., and Manisankar, P. (2014) Electroanalysis 26, 1958–1965.
[55] Sethuraman, V., Muthuraja, P., Raj, J.A., and Manisankar, P. (2016) Biosens. Bioelectron. 84, 112–119.
[56] Vicentini, F.C., Garcia, L.L., Figueiredo-Filho, L.C., Janegitz, B.C., and Fatibello-Filho, O. (2016) Enzyme Microb. Technol. 84, 17–23.
[57] Maleki, N., Kashanian, S., Maleki, E., and Nazari, M. (2017) Biochem. Eng. J. 128, 1–11.